Giant Cascaded Four-Wave Mixing Effect in Tapered Plasmonic Nanoantennas Embedded in a Nonlinear Dielectric Background

Ivan S. Maksymov[1,2,*], Andrey E. Miroshnichenko[2], and Yuri S. Kivshar[2]

[1]School of Physics, University of Western Australia, 35 Stirling Highway, Crawley WA 6009, Australia
[2]Nonlinear Physics Centre, Research School of Physics and Engineering,
Australian National University, Canberra ACT 0200, Australia
*corresponding author, E-mail: ivan.maksymov@uwa.edu.au

Abstract

We theoretically study the cascaded four-wave mixing (FWM) in a broadband tapered plasmonic nanoantenna embedded in a nonlinear indium-tin-oxide (ITO) background. In comparison with ITO without the nanoantenna, we demonstrate a 300–fold increase in nonlinear frequency conversion. This is achieved by tuning the elements of the nanoantenna to resonance frequencies involved in the cascaded FWM interaction.

1. Introduction

Modern nanophotonic devices such as, for example, nanoantennas [1] rely largely on optical properties of metals. However, the optical efficiency of high-quality metal nanostructures is often compromised by intrinsically high absorption losses in the metal.

Similar to metal nanostructures, dielectric nanostructures can have strong resonant behaviour at optical frequencies. Most significantly, dielectric nanostructures can virtually be loss-free and their optical properties are less affected by fabrication imperfections. These qualities make dielectric nanostructures very appealing for novel applications in nanophotonics such as, e.g., optical nanoantennas [2-4] and slot waveguides [5]. Nevertheless, dielectric nanoparticles cannot substitute metal nanostructures in a diverse range of fields including catalysis, sensing, photochemistry, medicine, and energy conversion [6].

In our previous works [7-9] we have shown that metal and dielectric nanostructures can work in tandem giving rise to novel functionalities for nanophotonic device applications. In this work, we demonstrate a giant cascaded FWM effect in a hybrid device consisting of a plasmonic nanoantenna embedded into a nonlinear ITO dielectric background [10].

2. Results and discussion

FWM is a nonlinear process transferring energy from a strong pump wave to waves upshifted and downshifted in frequency from the pump frequency. When a strong pump wave at the frequency ω_p and a weak signal wave at the frequency ω_s ($\omega_s > \omega_p$) propagate in a nonlinear medium, photons from these waves annihilate and new photons are created at the frequencies $\omega_1 = 2\omega_p - \omega_s$ and $\omega_2 = 2\omega_s - \omega_p$. Furthermore, the created waves participate further in the FWM process leading to the cascaded generation of waves at frequencies around ω_s and ω_p

$$\omega_- = 2\omega_{low} - \omega_{high};\ \omega_+ = 2\omega_{high} - \omega_{low} \qquad (1)$$

where ω_{low} and ω_{high} denote generated frequencies belonging to the low– and high–frequency sidebands.

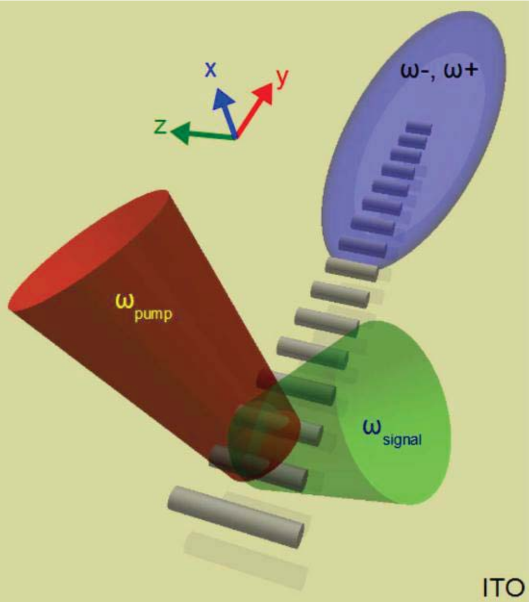

Figure 1: Illustration of the cascaded FWM conversion with a tapered nanoantenna. Two z–polarized waves (pump and signal) with different telecom frequencies that excite the nanoantenna surrounded by a nonlinear medium, ITO. A nanoantenna supports up to 10 frequencies on both sides of the pump frequency. Waves at these frequencies are emitted by the nanoantenna into a narrow cone in the y–direction.

Significant FWM occurs only if the phase mismatch nearly vanishes, which can be satisfied when the frequencies involved in FWM are close to each other. We meet the latter condition and, moreover, further boost the strength of cascaded FWM using a tapered nanoantenna (Fig. 1). We

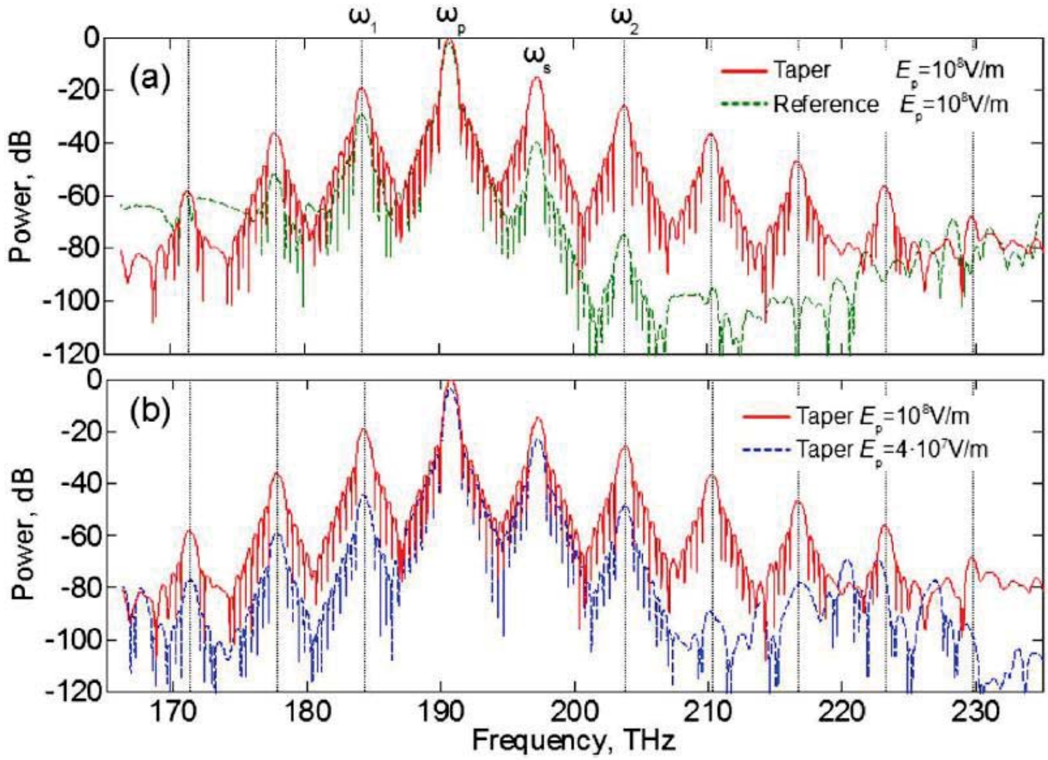

Figure 2: (a), (b) Far-field power spectra of the 21–element tapered nanoantenna (red solid curve, $E_p = 10^8$ V⁄m; blue dashed curve, $E_p = 4\times10^7$ V⁄m) and untapered reference structure (green dashed curve, 10^8 V⁄m). Straight dotted lines indicate frequencies generated due to FWM. All spectra are normalized to the peak value of the red curve.

embed the nanoantenna in a nonlinear ITO background and also gradually decrease the length of its silver elements in accord with Eq. (1) and optical properties of ITO [10].

The tuning of the operating band of the nanoantenna to the near-IR spectral region is achieved by rescaling the length of its elements as $L_{ITO} = L_{air}/\sqrt{\varepsilon_{ITO}}$, where L_{air} is the length of the elements of the same nanoantenna but suspended in air and ε_{ITO} is the dielectric constant of ITO. The choice of the rest of the parameters is dictated by the resolution attainable with current fabrication technologies [1]. The elements of the nanoantenna have the square cross-section of 50 nm per 50 nm and are separated by the spacing of 30 nm.

Using a customised three–dimensional nonlinear finite-difference time-domain method [11, 12], we investigate nonlinear characteristics of the tapered nanoantenna by exciting it with the pump wave at frequency 190.8 THz and the signal wave at 197.3 THz (both z–polarized, see Fig. 1). For the sake of clarity, we use two amplitudes of the pump wave: $E_p = 4\times10^7$ V⁄m and 10^8 V⁄m causing, correspondingly, nonlinear refractive index change of $\sim10^{-3}$ and $\sim5\times10^{-2}$ in the bulk ITO without the nanoantenna. The amplitude of the signal wave is equal to $0.1E_p$.

We simulate the far-field response of the nanoantenna by integrating the power flux through a plane perpendicular to the y–axis and located far beyond the nanoantenna front end. For the 21–element nanoantenna and $E_p = 10^8$ V⁄m [Fig. 2(a)] we observe the signal generation due to FWM in accord with Eq. (1). The tapered nanoantenna enhances the pump and signal waves as well as five generated waves above –50 dB in the low– and high–frequency bands. The enhancement is quantified by the frequency conversion efficiency calculated as $\eta = |P_c|/|P_s|$, where P_c is the power of the converted wave at $\omega_{-,+}$ and P_s is the power of the signal wave in the detected far-field. For example, for the converted waves at 184.3 THz and 203.8 THz, we obtain η = –4.2 dB and –11.2 dB, correspondingly.

A qualitatively similar picture is observed for the 21–element nanoantenna but excited with a weaker pump wave [Fig. 2(b)] for $E_p = 4\times10^7$ V⁄m, one obtains η = –22 dB and –33.7 dB. In contrast, only one peak above –50 dB is generated at ω_1 by the untapered reference structure consisting of 21 elements and tuned to resonate at ω_p by setting the element length to 200 nm.

To further quantify the rate of conversion efficiency enhancement, we also calculate η for an idealized case of plane wave propagation in ITO without the nanoantenna. We use an analytical asymptotic approximate formula that expresses η as a function of E_p after the propagation distance of the plane wave L [13]

$$\eta = (3\omega_p\chi^{(3)}E_p^2L/8nc)^2, \qquad (2)$$

where n is the linear refractive index of ITO, $\chi^{(3)}$ is the third-order susceptibility of ITO and c is the speed of light. In accord with Eq. (2), for $E_p = 4\times10^7$ V⁄m the conversion efficiency of −22 dB at 184.3 THz can be achieved if the plane wave propagates for more than 25 μm. By substituting the total length of the 21–element nanoantenna (~1.7 μm) into Eq. (2), we obtain $\eta_{ant}/\eta_{bulk} \approx 300$.

3. Conclusions

In comparison with ITO medium without the nanoantenna, we have demonstrated a 300−fold enhancement of the frequency conversion due to cascaded FWM in a plasmonic nanoantenna embedded in an ITO background. This is achieved due to a judicious choice of the number and length of nanoantenna elements in accord with the frequencies involved in FWM. Apart from potential applications in nonlinear plasmonic devices, our finding can be used to enhance parametric amplification of two pre-existing waves exciting the nanoantenna at frequencies ω_1 and ω_2.

Acknowledgements

This work was supported by the UPRF scheme of the University of Western Australia and the Australian Research Council.

References

[1] I.S. Maksymov, I. Staude, A.E Miroshnichenko, Yu.S. Kivshar, Optical Yagi-Uda Nanoantennas, *Nanophotonics* 1: 65−81, 2012.

[2] A. E. Krasnok, A. E. Miroshnichenko, P. A. Belov, and Yu. S. Kivshar, All-dielectric nanoantennas, *Opt. Express* 20: 20599−20604, 2012.

[3] A. E. Miroshnichenko and Yu. S. Kivshar, Fano resonances in all-dielectric oligomers, *Nano Lett.* 12: 6459-6463, 2012.

[4] A. E. Krasnok, I. S., Maksymov, A. I. Denisyuk, P. A. Belov, A. E. Miroshnichenko, C. R. Simovski and Yu. S. Kivshar, Optical nanoantennas, *Physics-Uspekhi* 1: 539−564, 2013.

[5] Q. Xu, V. R. Almeida, R. R. Panepucci, and M. Lipson, Experimental demonstration of guiding and confining light in nanometer−size low−refractive−index material, *Opt. Lett.* 29: 1626−1628, 2004.

[6] A. Desireddy, B. E. Conn, J. Guo, B. Yoon, R. N. Barnett, B. M. Monahan, K. Kirschbaum, W. P. Griffith, R. L. Whetten, U. Landman, and T. P. Bigioni, Ultrastable silver nanoparticles, *Nature* ,doi: 10.1038/nature12523

[7] F. De Angelis, M. Patrini, G. Das, I. Maksymov, M. Galli, L. Businaro, L. C. Andreani, and E. Di Fabrizio, A hybrid plasmonic−photonic nanodevice for label-free detection of a few molecules, *Nano Letters* 8: 2321−2327, 2008.

[8] F. De Angelis, G. Das, P. Candeloro, M. Patrini, M. Galli, A. Bek, M. Lazzarino, I. S. Maksymov, C. Liberale, L. C. Andreani, and E. Di Fabrizio, 3D Adiabatic compression of plasmon polaritons for nano−mapping at 10 nm resolution, *Nature Nanotechnology* 5: 67−72, 2010.

[9] I. S. Maksymov and Yu. S. Kivshar, Broadband light coupling to dielectric slot waveguides with tapered plasmonic nanoantennas, *Opt. Lett.* 38: 4853−4856, 2013.

[10] I. S. Maksymov, A. E. Miroshnichenko, and Yu. S. Kivshar, Cascaded four-wave mixing in tapered plasmonic nanoantenna, *Opt. Lett.* 38: 79−81, 3013.

[11] I.S. Maksymov, L.F. Marsal, and J. Pallarès, Finite−difference time−domain analysis of band structures in one−dimensional Kerr−nonlinear photonic crystals, *Opt. Commun.* 239: 213−222 2004.

[12] I.S. Maksymov, L.F. Marsal, M.A. Ustyantsev, and J. Pallarès, Band structure calculation in two-dimensional Kerr−nonlinear photonic crystals, *Opt. Commun.* 248: 469−477 2005.

[13] I. S. Maksymov, A. A. Sukhorukov, A. A. Lavrinenko and Yu. S. Kivshar, Comparative study of FDTD−adopted numerical algorithms for Kerr nonlinearities, *IEEE Antennas Wireless Propagation. Lett.* 10: 143−146, 2011.